Identifying Optimal Inorganic Nanomaterials for Hybrid Solar Cells

Hongjun Xiang* and Su-Huai Wei

National Renewable Energy Laboratory, Golden, Colorado 80401

Xingao Gong

Surface Science Laboratory and Department of Physics, Fudan University, Shanghai 200433, China

Received: August 17, 2009

As a newly developed photovoltaic technology, organic−inorganic hybrid solar cells have attracted great interest because of the combined advantages from both components. An ideal inorganic acceptor should have a band gap of about 1.5 eV and energy levels of frontier orbitals matching those of the organic polymer in hybrid solar cells. Hybrid density functional calculations are performed to search for optimal inorganic nanomaterials for hybrid solar sells based on poly(3-hexylthiophene) (P3HT). Our results demonstrate that InSb quantum dots or quantum wires can have a band gap of about 1.5 eV and highest occupied molecular orbital level about 0.4 eV lower than P3HT, indicating that they are good candidates for use in hybrid solar cells. In addition, we predict that chalcopyrite $MgSnSb_2$ quantum wire could be a low-cost material for realizing high-efficiency hybrid solar cells.

Introduction

In view of the limited availability of fossil fuels and the disastrous environmental issues concomitant with their combustion, it is imperative to develop renewable energy resources for the increasing global energy demand. Among the possibilities, solar energy conversion is of great interest because it is globally available and inexhaustible, and electrical energy can be converted to other energy currencies such as hydrogen. High efficiencies above 20% have been achieved by monocrystalline silicon solar cells; however, their production cost and energy consumption during the fabrication process are quite high. Therefore, the development of inexpensive solar cells is of growing interest.

Organic polymer-based photovoltaics have been considered as a new alternative photovoltaic technology due to their flexibility, light weight, low-cost fabrication, easy integration into a wide variety of devices, and tunable properties of organic materials. Bulk heterojunction (BHJ) solar cells based on intimate blends of polymer donor and acceptor materials are of particular interest. Recently,[1,2] the BHJ solar cells have achieved power conversion efficiency (PCE) of about 5% where poly(3-hexylthiophene) (P3HT), with an optical band gap of 1.9 eV, acts as a photon absorber and a donor and a fullerene derivative PCBM ([6,6]-phenyl-C_{61}-butyric methyl ester) acts as an acceptor. However, there are some limitations in the P3HT/PCBM blend solar cells: low charge mobility, weak absorption in the visible spectrum, and low open-circuit voltage (V_{oc}) (about 0.6 V[1,2]) due to the extremely deep-lying lowest unoccupied molecular orbital (LUMO) levels of PCBM. One of the common approaches to increasing the spectral breadth of absorbed photons is the use of so-called low-band-gap (less than 1.5 eV) polymers.[3] Unfortunately, low-band-gap polymer-based BHJ solar cells have achieved efficiency no more than 3.5% so far.

As an alternative polymer-based photovoltaic cell, the organic−inorganic hybrid solar cell is promising because of the advantages resulting from two types of materials with low cost and easy preparation from organic material, high electron mobility, excellent chemical and physical stability, size tunability, and complementary light absorption from the inorganic semiconductors. Various hybrid solar cells have been reported, including devices that utilize polymer in conjunction with CdSe,[4] ZnO,[5] TiO_2,[6] PbSe,[7] $CuInS_2$,[8] and Si[9] spherical nanocrystals. In addition, Huynh et al.[10] made hybrid solar cells based on CdSe nanorods because their one-dimensional nature can provide a rapid continuous transport path for charge carriers. In particular, hybrid solar cells based on hyperbranched CdSe (the band gap of bulk CdSe is about 1.8 eV) nanocrystals hold the efficiency record (2.2%) for hybrid devices.[11] Air-stable polymer photovoltaics were demonstrated by replacing fullerenes with ZnO nanoparticles.[12] In addition, Bredol et al.[13] showed that a high V_{oc} (1.2 V) can be achieved in a system prepared from P3HT in contact with ZnS nanoparticles (band gap of ca. 4 eV). However, the efficiency is rather low (0.2%), partly due to the negligible contribution to the photocurrent from ZnS. Bilayer heterojunction hybrid solar cells using low-band-gap semiconductors such as PbS nanoparticles to enhance the light harvest[14] were fabricated, but the V_{oc} is rather limited (0.35 V). In order to maximize the efficiency of hybrid solar cells, it is imperative to increase not only the open-circuit voltage V_{oc} but also the short-circuit current I_{sc}. Therefore, it is desirable to find an inorganic acceptor material that can absorb photons in the solar spectrum efficiently for larger I_{sc} and possesses a higher-lying LUMO level for higher V_{oc} .

In this paper, we identify some semiconducting quantum dots/wires that are optimal for use as the inorganic component in hybrid solar cells, in the sense that both high V_{oc} and good visible absorption could be achieved in the same time.

Computational Methods

In order to find electron-accepting and -conducting materials with a better match, one needs to know the energy of their levels involved in the photovoltaic process on an absolute scale [highest occupied molecular orbital (HOMO) and LUMO

* Corresponding author.

10.1021/jp907942p CCC: $40.75
Published on Web 10/01/2009

relative to the vacuum level]. It is well-known that local density approximation (LDA)[15] in the density functional theory (DFT) seriously underestimates the band gaps of semiconductors, and the absolute band edge energy from the LDA calculation is not always reliable. Recently, a hybrid density functional,[16] which incorporates a fraction α of Hartree−Fock exchange, was found[17] to predict band offsets at semiconductor−oxide interfaces in excellent agreement with experiment. Hereafter, we will employ the hybrid density functional to calculate the HOMO and LUMO level of all materials. Following the method of Alkauskas et al.,[17] the fraction α in the hybrid functional is tuned to reproduce the experimental band gap. For structural relaxations, the LDA is adopted because of its high accuracy and efficiency in geometrical optimizations. The vacuum level is defined as the average electrostatic potential in the vacuum region where it approaches a constant, as in the work function calculation.[18] DFT calculations were performed by the projected augmented wave (PAW) method[19] as implemented in the Vienna ab initio simulation package (VASP).[20]

Results and Discussion

P3HT. P3HT[21,22] is widely used as a light-harvesting material in organic solar cells because it is an effective hole transport material in its regioregular form, demonstrating the highest field-effect hole mobilities observed in known polymers. Here in this work, we will use P3HT as the organic component of the hybrid solar cells, as most experimentalists did.[9,10] As a first step, we calculate the HOMO and LUMO of regioregular P3HT. For P3HT, the hybrid functional calculation with $\alpha = 0.28$ gives a direct band gap of 2.22 eV, which is very close to its experimental electronic band gap (2.2 eV) from electrochemical data.[23] The calculated HOMO and LUMO levels of P3HT relative to the vacuum level are −4.43 and −2.21 eV, respectively.

InSb and InAs. It is well-known that crystalline semiconductor solar cells that best match the solar spectrum have a band gap of ≃1.5 eV. Similar to the requirement of an optimal low-band-gap polymer,[3] we propose that the optimal low-band-gap inorganic semiconductor should have a direct band gap of about 1.5 eV and a HOMO level about 0.3 eV below that of P3HT (see Figure 1). The 0.3 eV energy difference can ensure effective exciton splitting and charge dissociation.[3,24] A larger energy difference would lead to wasted energy that does not contribute to the device performance.[25] With this ideal hybrid solar cell, we can achieve a theoretical V_{oc} of 1.2 V.

Besides the requirements of an optimal inorganic semiconductor nanomaterial shown in Figure 1, the material should be nontoxic and should have a direct band gap. After a survey of low-band-gap semiconductors, we find that some III−V semiconductors might be good candidates for optimal inorganic nanomaterials: InSb and InAs are direct band-gap semiconductors with experimental band gaps of 0.26 and 0.42 eV, respectively. For these bulk zinc-blende structures, both the valence band maximum (VBM) and conduction band minimum (CBM) are located at Γ. In the absence of spin−orbit coupling (SOC), the VBM (Γ_{15v}) is triply degenerate (not counting spin degeneracy), and the CBM (Γ_{1c}) is nondegenerate (see Figure 2a). Because these compounds are composed of heavy elements, there are substantial changes on the valence band due to the relativistic effect, that is, spin−orbit coupling (SOC). As can be seen from Figure 2, SOC splits the Γ_{15v} state into a high-lying 4-fold degenerate Γ_{8v} state and a low-lying 2-fold degenerate Γ_{7v} state. Defining the spin−orbit splitting between the Γ_{8v} state and the Γ_{7v} state as Δ_{so}, the Γ_{8v} state has a higher

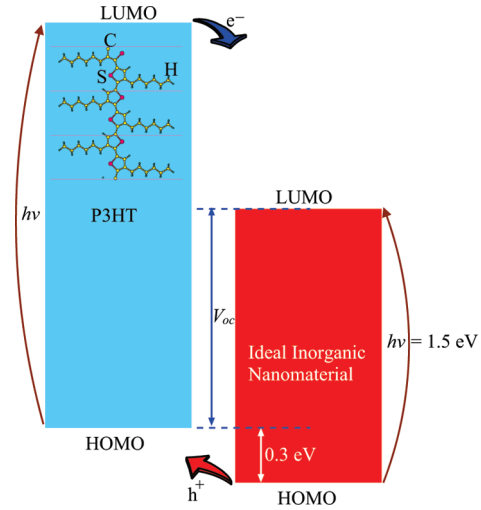

Figure 1. Schematic illustration of the requirement for an ideal inorganic nanomaterial to be used in hybrid solar cells. The ideal inorganic nanomaterial should have a band gap of about 1.5 eV for light harvesting and a HOMO level that is lower by about 0.3 eV than that of the donor for facilitating the hole transfer. (Inset) Structure of P3HT.

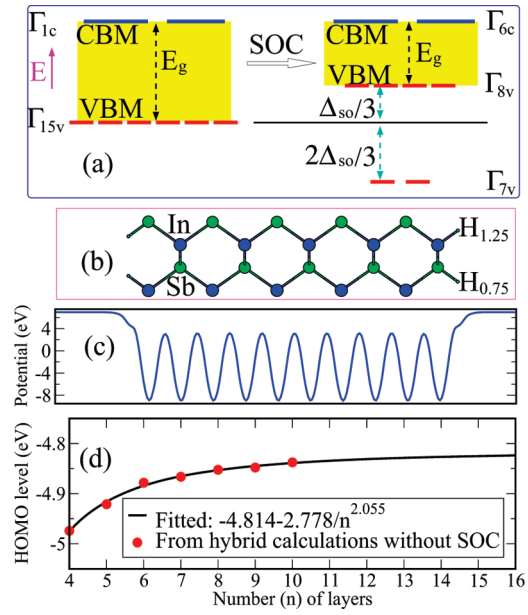

Figure 2. (a) Schematic illustration of the effect of SOC on the CBM and VBM of zinc-blende semiconductors. (b) Structure of a 10-layer [110] InSb slab. (c) Planar average of total local potential of the 10-layer [110] InSb slab shown in panel b. (d) HOMO levels of [110] InSb slabs from the hybrid calculations without SOC. The solid line is the fitted result.

energy than the original Γ_{15v} state by about $\Delta_{so}/3$ to a first-order approximation, and SOC does not change the energy of the Γ_{1c}-derived Γ_{6c} state. Therefore, the band gap (HOMO level) is decreased (increased) by $\Delta_{so}/3$: $E_g(\text{SOC}) = E_g(\text{no SOC}) - \Delta_{so}/3$, and $E_{\text{HOMO}}(\text{SOC}) = E_{\text{HOMO}}(\text{no SOC}) + \Delta_{so}/3$. The calculated Δ_{so} values for bulk InSb and InAs are shown in Table 1. We find good agreement with previous theoretical[26] and experimental results.[27] The fractions α in the hybrid functional, which reproduce the experimental band gaps, and theoretical band gaps for bulk InSb and InAs, are also listed in Table 1.

Experimentally, the surfaces of semiconductor nanomaterials are usually passivated, as indicated by the Fourier transform infrared spectroscopic study on Si nanocrystal-based hybrid solar

TABLE 1: Calculated Spin−Orbit Splitting (Δ_{so}), Fraction Parameters (α) Used in the Hybrid Calculations, Band Gaps (E_g), and HOMO Levels (E_{HOMO}) for InSb, InAs, and $MgSnSb_2$[a]

	Δ_{so} (eV)	α	E_g	E_{HOMO} (eV)
InSb	0.760	0.120	0.268	−4.561
InAs	0.361	0.135	0.414	−4.968
$MgSnSb_2$	0.709	0.145	1.027	−4.668

[a] The band gaps and HOMO levels have included the SOC effect and correction to the LDA error. The HOMO level refers to that of the passivated infinite nanocrystal extrapolated from the results from the slab calculations. The α values in the hybrid functional are tuned to reproduce the experimental band gaps of semiconductors, except that the α value for $MgSnSb_2$ is taken to be the mean of the α value for InSb and that for AlSb.

cells.[9] We now estimate the HOMO levels of passivated InSb and InAs nanocrystals of various sizes. Because direct calculation of the absolute energy levels of a bulk system is impossible due to the uncertain constant in the periodic electrostatic potential, here we try to extrapolate the HOMO levels of passivated nanocrystals with infinitely large size through fitting to the results of a series of finite slab systems. In the following, we will take InSb as an example to illustrate how this is done. We consider the most stable nonpolar [110] surface slabs: A 10-layer InSb [110] slab is shown in Figure 2b for reference. The surfaces are fully passivated by pseudohydrogen atoms.[28] The vacuum region (about 10 Å) between neighboring slabs is so large that there is almost no interaction between them, as can be seen from the plot of the planar average of the local potential (see Figure 2c). We calculate the HOMO levels for [110] slabs with thickness ranging from 4 to 10 layers. The HOMO levels from the hybrid functional calculations (α = 0.120) without SOC are plotted in Figure 2. We can see that the decrease of HOMO levels due to the quantum confinement effect is not very large. As a matter of fact, the HOMO levels decrease much slower than the increase of LUMO levels: the band gap increases 0.73 eV, whereas the HOMO level decreases only about 0.14 eV from the 10- to the 4-layer slab. The small quantum confinement effect on the HOMO is a consequence of a large hole effective mass. Fitting the HOMO levels as a function of the number (n) of layers results in the following experssion: E_{HOMO}(no SOC) = $-4.81 - 2.78/n^{2.06}$ eV. The exponent (2.06) is very close to that (2.0) from the effective mass approximation. Therefore, the calculated HOMO level for the passivated InSb cluster with infinitely large size after inclusion of SOC will be −4.56 eV. In a similar way, we find that the calculated HOMO level for InAs infinite nanocrystals is −4.97 eV. InAs nanocrystals have a lower HOMO level than InSb nanocrystals because the As 4p orbital lies below the Sb 5p orbital.

It is well-known that the quantum confinement effect decreases (increases) the HOMO (LUMO) level of the semiconducting nanocrystals and thus enlarges the band gap. Therefore, the InAs nanocrystal will have a much lower HOMO level (lower than −4.97 eV) than that (−4.43 eV) of P3HT, and thus it is not a good choice for use in hybrid solar cells. InSb nanocrystals appear to be promising for use in hybrid solar cells because the HOMO level of infinite InSb nanocrystals is lower by 0.13 eV than that of P3HT. Hereafter, we will identify the best InSb quantum wires and dots that satisfy the requirements for the ideal inorganic nanomaterial (Figure 1). We consider several InSb quantum wires (QW) in the [111] growth direction with hexagonal cross sections. The diameters of the QW range from 1.2 to 3.2 nm. [The effective diameter of QW is defined in terms of the number of atoms (not counting the surface pseudo-H atoms) in a wire.[29]] The LDA results without SOC are shown in Figure 3a. We can see that the band gaps (HOMO levels) decrease (increase) with increasing diameters, as expected. Because doing hybrid functional calculations on large QW is a forbidden task, we will estimate the HOMO levels and band gaps of large QW. From the [110] InSb slab calculations, we find that the LDA functional overestimates the absolute HOMO level of infinite InSb nanocrystal by 0.180 eV and underestimates the band gap of bulk InSb by 0.80 eV. Hybrid functional (α = 0.120) calculations on QW with diameters of 1.2 and 1.5 nm show that the correction on the LDA band gap and HOMO levels depends little on the diameter of QW, as shown in Figure 3a. For simplicity, the corrections on the band gap and HOMO levels from the LDA calculations without SOC for all InSb nanostructures are taken to be $0.80 - \Delta_{so}/3 = 0.54$ and $-0.18 + \Delta_{so}/3 = 0.07$ eV, respectively. The final predicted band gap and HOMO levels for all four QW are shown in Figure 3a. We can deduce that a InSb QW with a diameter of 2 nm would have a band gap of 1.50 eV and a HOMO level of −4.86 eV, which is about 0.43 eV lower than the calculated P3HT HOMO level; thus it appears to be a good choice (see Figure 1) for the use in hybrid solar cells. We also calculate the band gaps and HOMO levels of spheric quantum dots (QD) with diameters ranging between 1.3 and 3.9 nm by use of the LDA. Similarly, they display a quantum confinement effect. After making corrections due to the LDA error and SOC, we find that a InSb QD with a diameter of 3.5 nm would have a band gap of 1.50 eV and a HOMO level about 0.50 eV below the calculated P3HT HOMO level. Therefore, InSb QD with diameters around 3.5 nm could also be used as the inorganic component in hybrid solar cells.

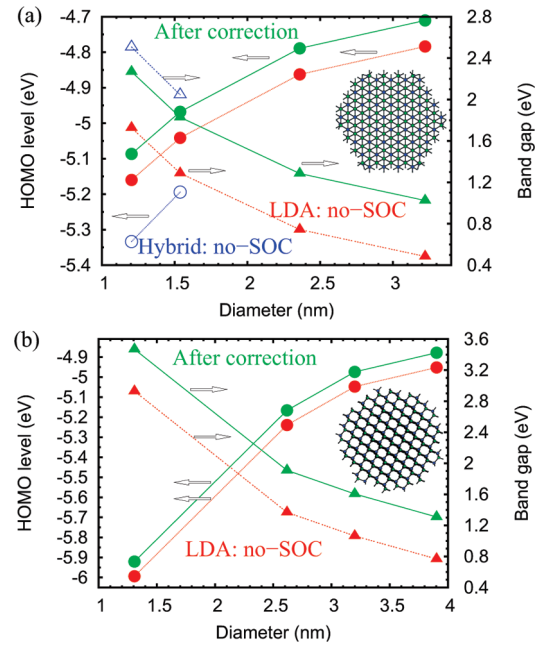

Figure 3. (a) Band gaps and HOMO levels of different [111] hexagonal InSb QW from LDA calculations without SOC, from hybrid functional calculations without SOC, and after corrections. (Inset) Top view of InSb QW with a diameter of about 3.6 nm. (b) Band gaps and HOMO levels of different spherical InSb QD from LDA calculations without SOC and after LDA + SOC corrections. (Inset) Structure of InSb QD with a diameter of about 3.9 nm.

$MgSnSb_2$. Above we have shown that InSb nanocrystals could be good candidates for use in hybrid solar cells. However, large-scale application might be unlikely because of the high

cost due to scarcity of In. To seek alternative materials, we consider ternary alloys where In is replaced with other metal elements. An immediate possibility would be replacing half of In with Cd and the other half with Sn. However, the toxicity of Cd will cause environmental problems. Therefore, we choose $ZnSnSb_2$ and $MgSnSb_2$ as possible candidates. Both $ZnSnSb_2$ and $MgSnSb_2$ should crystallize into the chalcopyrite lattice. Test calculations show that infinite $ZnSnSb_2$ nanocrystal has a relatively high HOMO level due to the large p−d repulsion between Sb 5p and high-lying Zn 3d orbitals, indicating that $ZnSnSb_2$ nanomaterials are not suitable for the inorganic acceptor. In the following, we will focus on $MgSnSb_2$. To predict the band gap of $MgSnSb_2$, we perform hybrid functional calculations with $\alpha = 0.145$, which is the mean of the α value (0.120) for InSb and that (0.170) for AlSb. This calculation gives a direct band gap of 1.26 eV for $MgSnSb_2$ before inclusion of SOC. After consideration of the SOC spliting ($\Delta_{so} = 0.71$ eV), the predicted band gap of $MgSnSb_2$ is 1.03 eV. The band gap value is larger than that (0.26 eV) of InSb. The two main reasons for the band gap increase are first, Mg 3s level is higher than In 5s levels, leading to a higher CBM for $MgSnSb_2$, and second, the p−d repulsion between unoccupied Mg 3d and occupied Sb 5p orbitals lowers the VBM in $MgSnSb_2$; in contrast, the p−d repulsion between occupied In 4d and occupied Sb 5p orbitals raises the VBM in InSb. Calculations on several [110] $MgSnSb_2$ nonpolar slabs show that the HOMO level (after corrections) is −4.67 eV, which is about 0.1 eV lower than that of InSb as explained above. To see whether $MgSnSb_2$ nanocrystals could be good acceptors in hybrid solar cells, we calculate the electronic structures of $MgSnSb_2$ QW of size about 3.5 nm. The passivated QW with a near-square cross section is along the [100] direction and enclosed by nonpolar {110} facets, as shown in Figure 4a. Our result indicates that the QW is a quasidirect band-gap semiconductor: LDA calculations without SOC give a direct band gap of 0.72 eV at Γ and an indirect band gap of 0.70 eV between VBM at Γ and CBM at $X = (0, 0, 0.5)$. The fact that the CBM is located at X instead of Γ is a consequence of the larger quantum confinement effect at Γ due to the smaller electron effective mass at Γ. The quasidirect nature of the band structure might reduce charge recombination and ensure minimal energy loss after photoexcitation. After correction of the LDA error and inclusion of the SOC effect, the direct band gap and HOMO level are 1.37 and −4.77 eV, respectively. We note that the fact that the direct gap is slightly smaller than 1.5 eV might not be a disadvantage: on one hand, the theoretical open-circuit voltage V_{oc} is still large (1.00 eV) because of the perfect position of the HOMO level; on the other hand, the smaller band gap increases the absorption of the low-energy photons. The absorption spectrum from the LDA calculation is shown in Figure 4b. The band-gap error is corrected by use of a scissor operator. We can see that the absorption beyond the direct band gap is continuous and strong, indicating that $MgSnSb_2$ QW are good light-harvesting materials. Therefore, our results show that $MgSnSb_2$ QW could be used in hybrid solar cells.

Conclusion

In summary, we propose that an ideal inorganic acceptor should have a band gap of about 1.5 eV and energy levels of frontier orbitals matching with the organic polymer in hybrid solar cells. Hybrid density functional calculations are performed to search for optimal inorganic nanomaterials for hybrid solar sells based on P3HT. Our results suggest that InSb quantum dots or quantum wires can have a band gap of about 1.5 eV and highest occupied molecular orbital level about 0.4 eV lower than P3HT and thus are good candidates. In addition, we predict that chalcopyrite $MgSnSb_2$ QW could be a cost-effective material for realizing high-efficiency hybrid solar cells.

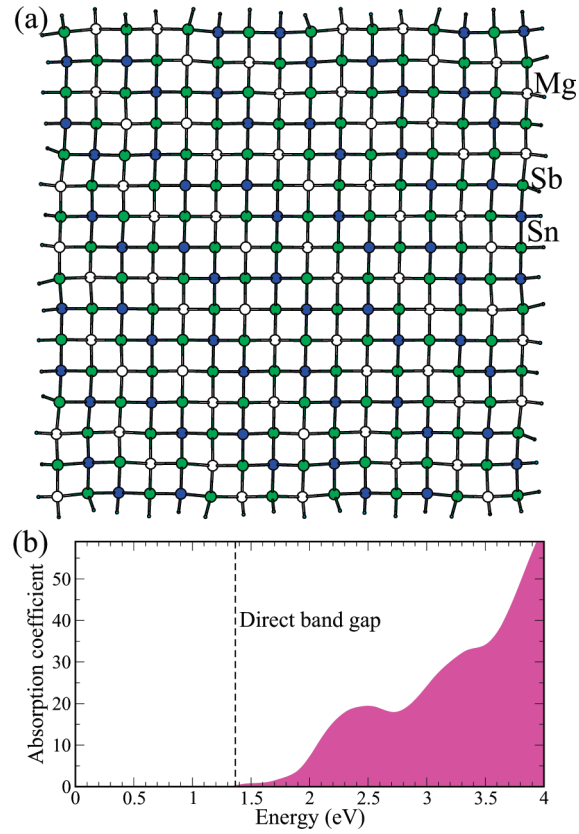

Figure 4. (a) Top view of passivated $MgSnSb_2$ QW with 3.5 nm × 3.5 nm cross section. The QW is along the [100] direction and enclosed by nonpolar 110 facets. (b) Theoretical absorption spectrum of $MgSnSb_2$ QW from the LDA calculation. A scissor operator is applied to correct the band-gap error. We use 0.1 eV broadening in calculating the spectrum. We assume that the incoming light polarization vector is along the QW direction.

Acknowledgment. We acknowledge useful discussion with Junwei Luo. This work is supported by the U.S. Department of Energy, under Contract DE-AC36-08GO28308.

References and Notes

(1) Ma, W.; Yang, C.; Gong, X.; Lee, K.; Heeger, A. J. *Adv. Funct. Mater.* **2005**, *15*, 1617.
(2) Li, G.; Shrotriya, V.; Huang, J. S.; Yao, Y.; Moriarty, T.; Emery, K; Yang, Y. *Nat. Mater.* **2005**, *4*, 864.
(3) Thompson, B. C.; Fréchet, J. M. J. *Angew. Chem., Int. Ed.* **2008**, *47*, 58.
(4) Greenham, N. C.; Peng, X.; Alivisatos, A. P. *Phys. Rev. B* **1996**, *54*, 17628.
(5) Beek, W. J. E.; Wienk, M. M.; Janssen, R. A. J. *Adv. Funct. Mater.* **2006**, *16*, 1112.
(6) Kwong, C. Y.; Choy, W. C. H.; Djurisiić, A. B.; Chui, P. C.; Cheng, K. W.; Chan, W. K. *Nanotechnology* **2004**, *15*, 1156.
(7) Cui, D.; Xu, J.; Zhu, T.; Paradee, G.; Ashok, S.; Gerhold, M. *Appl. Phys. Lett.* **2006**, *88*, 183111.
(8) Arici, E.; Sariciftci, N. S.; Meissner, D. *Adv. Funct. Mater.* **2003**, *13*, 165.
(9) Liu, C.; Holman, Z. C.; Kortshagen, U. R. *Nano Lett.* **2009**, *9*, 449.
(10) Huynh, W. U.; Dittmer, J. J.; Alivisatos, A. P. *Science* **2002**, *295*, 2425.
(11) Gur, I.; Fromer, N. A.; Chen, C. P.; Kanaras, A. G.; Alivisatos, A. P. *Nano Lett.* **2007**, *7*, 409.
(12) Krebs, F. C. *Sol. Energy Mater. Sol. Cells* **2008**, *92*, 715.

(13) Bredol, M.; Matras, K.; Szatkowski, A.; Sanetra, J.; Prodi-Schwab, A. *Sol. Energy Mater. Sol. Cells* **2009**, *93*, 662.
(14) Günesa, S.; Fritz, K. P.; Neugebauer, H.; Sariciftci, N. S.; Kumar, S.; Scholes, G. D. *Sol. Energy Mater. Sol. Cells* **2007**, *91*, 420.
(15) (a) Perdew, J. P.; Zunger, A. *Phys. Rev. B* **1981**, *23*, 5048. (b) Ceperley, D. M.; Alder, B. J. *Phys. Rev. Lett.* **1980**, *45*, 566.
(16) Perdew, J. P.; Ernzerhof, M.; Burke, K. *J. Chem. Phys.* **1996**, *105*, 9982.
(17) Alkauskas, A.; Broqvist, P.; Devynck, F.; Pasquarello, A. *Phys. Rev. Lett.* **2008**, *101*, 106802.
(18) Shan, B.; Cho, K. *Phys. Rev. Lett.* **2005**, *94*, 236602.
(19) (a) Blöchl, P. E. *Phys. Rev. B* **1995**, *50*, 17953. (b) Kresse, G.; Joubert, D. *Phys. Rev. B* **1999**, *59*, 1758.
(20) (a) Kresse, G.; Furthmüller, J. *Comput. Mater. Sci.* **1996**, *6*, 15. (b) Kresse, G.; Furthmüller, J. *Phys. Rev. B* **1996**, *54*, 11169.
(21) Kanai, Y.; Grossman, J. C. *Nano Lett.* **2007**, *7*, 1967.
(22) Dag, S.; Wang, L. W. *Nano Lett.* **2008**, *8*, 4185.
(23) Heeney, M.; Zhang, W.; Crouch, D. J.; Chabinyc, M. L.; Gordeyev, S.; Hamilton, R.; Higgins, S. J.; McCulloch, I.; Skabara, P. J.; Sparrowe, D.; Tierney, S. *Chem. Commun.* **2007**, 5061.
(24) Brabec, C. J.; Winder, C.; Sariciftci, N. S.; Hummelen, C.; Dhanabalan, A.; von Hal, P. A.; Janssen, R. A. J. *Adv. Funct. Mater.* **2002**, *12*, 709.
(25) Koster, L. J. A.; Milhailetchi, V. D.; Blom, P. W. M. *Appl. Phys. Lett.* **2006**, *88*, 093511.
(26) Carrier, P.; Wei, S.-H. *Phys. Rev. B* **2004**, *70*, 035212.
(27) *Semiconductors: Data Handbook*; Madelung, O., Ed.; Springer: Berlin and Heidelberg, Germany, 2004.
(28) Xiang, H. J.; Wei, S.-H. *Nano Lett.* **2008**, *8*, 1825.
(29) Li, J.; Wang, L. W. *Chem. Mater.* **2004**, *16*, 4012.

JP907942P